AGU100 ADVANCING EARTH AND SPACE SCIENCE

Geophysical Research Letters

RESEARCH LETTER
10.1029/2018GL079344

Key Points:
- Tectonic tremor can be used to constrain physical parameters for use in GMPEs where moderately sized earthquakes occur infrequently
- Inversion of tectonic tremor data indicates that seismic wave attenuation varies along strike in Cascadia
- Frequency-dependent attenuation from tectonic tremor is observed to be consistent with models developed using moderate-to-large earthquakes

Supporting Information:
- Supporting Information S1

Correspondence to:
G. F. Littel,
geenalittel10@gmail.com

Citation:
Littel, G. F., Thomas, A. M., & Baltay, A. S. (2018). Using tectonic tremor to constrain seismic wave attenuation in Cascadia. *Geophysical Research Letters*, *45*, 9579–9587. https://doi.org/10.1029/2018GL079344

Received 22 JUN 2018
Accepted 8 SEP 2018
Accepted article online 13 SEP 2018
Published online 27 SEP 2018

Using Tectonic Tremor to Constrain Seismic Wave Attenuation in Cascadia

Geena F. Littel[1], Amanda M. Thomas[1], and Annemarie S. Baltay[2]

[1]Department of Earth Sciences, University of Oregon, Eugene, OR, USA, [2]Earthquake Science Center, USGS Menlo Park, Menlo Park, CA, USA

Abstract Tectonic tremor can be used to constrain seismic wave attenuation for use in ground motion prediction equations in regions where moderately sized earthquakes occur infrequently. Here we quantify seismic wave attenuation by inverting tremor ground motion amplitudes in different frequency bands of interest, to determine frequency dependence of and spatial variations in seismic wave attenuation in Cascadia. Due to the density of tremor data, we are able to resolve along-strike variations in the attenuation parameter. We find that tectonic tremor exhibits the frequency dependence expected for attenuation, as determined from ground motion prediction equations developed from moderate-to-large magnitude earthquakes. This implies that attenuation along these paths is independent of the source mechanism. This study demonstrates that tectonic tremor can be used to provide insight into the physical factors responsible for attenuation and to refine estimates of attenuation for ground motion prediction, thus having important implications for hazard assessment and engineering seismology.

Plain Language Summary Earthquake ground motion models use estimates of seismic wave attenuation, that is, the decrease in amplitude of a seismic wave along its path from the earthquake source. Seismic wave attenuation is typically determined by analyzing ground motion from moderate-to-large earthquakes. Yet Cascadia also hosts tremor, a group of many small seismic signals accompanying slow sliding of the subducting plate. Because tremor occurs frequently when compared to regular earthquakes in Cascadia, it presents an opportunity to better refine attenuation parameters for use in ground motion models. We quantify seismic wave attenuation using tremor ground motion amplitudes to determine the extent of regional variations and frequency dependence of seismic wave attenuation in Cascadia. Incorporating spatial modifications and allowing for varying frequencies would increase the accuracy of the ground motion model. We are able to resolve spatial variations in the attenuation parameter along strike in Cascadia and observe the frequency dependence expected for attenuation, as seen in ground motion models developed from moderate-to-large magnitude earthquakes. Hence, we show that tectonic tremor can be used to provide insight into the physical factors responsible for attenuation and refine estimates of attenuation for ground motion models, thus having important implications for seismic hazard assessment. This is especially helpful in regions where moderate-to-large earthquakes are sparse, such as Cascadia.

1. Introduction

Geologic and historical evidence indicates that the Cascadia Subduction Zone experienced a large ($M_w \geq 8$) megathrust earthquake in 1700 (Atwater, 1995; Satake et al., 1996, 2003). Its estimated several hundred year recurrence interval (Atwater et al., 2014; Goldfinger et al., 2012) heightens interest in understanding the seismic hazard in the Pacific Northwest. Hazard analyses employ ground motion prediction equations (GMPEs), which relate the ground motion at a site to source, path, and site parameters, determined empirically from earthquake ground motion data (e.g., Petersen et al., 2014). The anelastic attenuation parameter in GMPEs describes the reduction in seismic wave amplitude along its path. Moderate to large (i.e., $M_w \sim 3–8$) earthquakes are typically used to constrain attenuation in GMPEs (e.g., Atkinson, 1995); however, the infrequent occurrence of intermediate-sized earthquakes in Cascadia limits the amount of data that can be used to determine attenuation.

Like many subduction zones worldwide, Cascadia exhibits slow, nearly aseismic earthquakes (Dragert et al., 2001; Miller et al., 2002). These are accompanied by groups of thousands of small, weak seismic signals, known

individually as low-frequency earthquakes (LFEs) and as a whole referred to as tectonic tremor (Obara, 2002; Shelly et al., 2007). In Cascadia, the coupled phenomenon, *episodic tremor and slip* (ETS), occurs periodically in ~10- to 19-month recurrence intervals (Rogers & Dragert, 2003). LFEs are inherently different from regular earthquakes because they are thought to originate from shear slip near the plate interface downdip of the seismogenic zone, have a characteristic frequency content of ~1–10 Hz, and moment-duration scaling distinct from that of regular earthquakes (Bostock et al., 2015; Ide et al., 2007; Obara, 2002; Royer & Bostock, 2014; Shelly et al., 2007). These earthquakes are called *low frequency* due to their depletion in high-frequency energy content. Yet their typical frequency range of several Hertz is considered high frequency (i.e., >1 Hz) in applications of ground motion modeling (e.g., Hanks & McGuire, 1981). Recognizing that the predominant frequencies of 1–10 Hz in tremor are relevant to applications in earthquake engineering, Baltay and Beroza (2013) used tectonic tremor data in an inversion to solve for a single average anelastic attenuation parameter in Cascadia. Using the same method, Yabe et al. (2014) found that attenuation parameters vary between subduction zones worldwide and that the upper crust is more attenuating than the lower crust.

Several studies have estimated attenuation within the Cascadia forearc by means of the quality factor, Q. For example, Bostock et al. (2017) estimated Q for southern Vancouver Island based on saturation frequency estimates from intraslab and deeper crustal earthquakes (depth > 20 km; see their Figure 7), focusing on the effects of near-source attenuation in the tremor source region. They find a frequency-independent Q that is similar for crustal and intraslab events and a lower frequency-dependent Q for crustal events. Gomberg et al. (2012) analyzed spectral decay rates of small earthquakes in the Olympic Peninsula, allowing them to estimate a regionally averaged, frequency-independent shear wave quality factor $Q_s = 200$. Fatehi and Hermann (2008) studied high-frequency (i.e., 0.16–25 Hz) ground motions in the Pacific Northwest and California, finding variations in attenuation relations between the two regions (reference is their Figure 1) using a frequency-dependent Q and distance-dependent geometrical spreading term.

Here we apply the method of Baltay and Beroza (2013) to tremor data from three different ETS episodes recorded in the Cascadia subduction zone to determine if and how the attenuation parameter varies spatially and with frequency. We use data filtered in varying bandwidths and compare our results with previous models of attenuation in GMPEs for Cascadia. We then solve for a spatially varying attenuation parameter and consider our results in context of the geologic setting of Cascadia.

2. Methods

Data are obtained and processed according to Baltay and Beroza (2013). We select three ETS episodes in 2009, 2012, and 2015–2016 to maximize the spatial distribution of events along strike (Figure 1). Individual tremor (LFE) epicenters and times are obtained from the Pacific Northwest Seismic Network online tremor catalog (Wech & Creager, 2008). Ground motion data are requested from the IRIS Data Management Center. Tremor data are 1-min continuous velocity waveforms recorded on each horizontal and vertical components of Plate Boundary Observatory borehole stations, corrected for instrument response. We use the Plate Boundary Observatory network only to ensure consistency throughout the study and because the borehole stations have a high signal-to-noise ratio. Velocity data are differentiated to acceleration and filtered in the 1- to 10-Hz frequency band, the predominant range of radiated energy from tremor (Bostock et al., 2015; Obara, 2002; Rogers & Dragert, 2003). Next, we take the peak amplitude over each 1-min window to define the peak-ground acceleration (PGA) used in the inversion. As tremor is considered to originate at the subducting plate interface (Brown et al., 2009; Shelly et al., 2006), we estimate hypocentral depths for individual LFEs using the McCrory et al. (2012) Juan de Fuca slab model (Figure 1). Additionally, daytime amplitudes are consistently larger than those at night (Figure 2a), likely due to anthropogenic noise. Therefore, we limit our data set to a 7-hr nighttime window (20:00–03:00 PST), consistent with Baltay and Beroza (2013). With PGA amplitudes on the scale of $\sim 1 \times 10^{-6}$ g, many records are near, or even below, common noise levels at large distances. We further limit our data set to the top 10% of events with the largest amplitudes. Finally, both Yabe et al. (2014) and Baltay and Beroza (2013) find that the determined attenuation is dependent on the hypocentral distance of recordings used, in that recordings at farther distances saturate at the noise floor. Thus, use of farther events yields a smaller attenuation value. A stable solution was found by including distances $\leq$ 150 km; therefore, to be consistent with their methods, we employ the same hypocentral distance threshold.

Following the inversion scheme of Baltay & Beroza, (2013; see supporting information Text S1), we first determine a path-averaged anelastic attenuation parameter for the entire data set (Figure 2b). We model ground

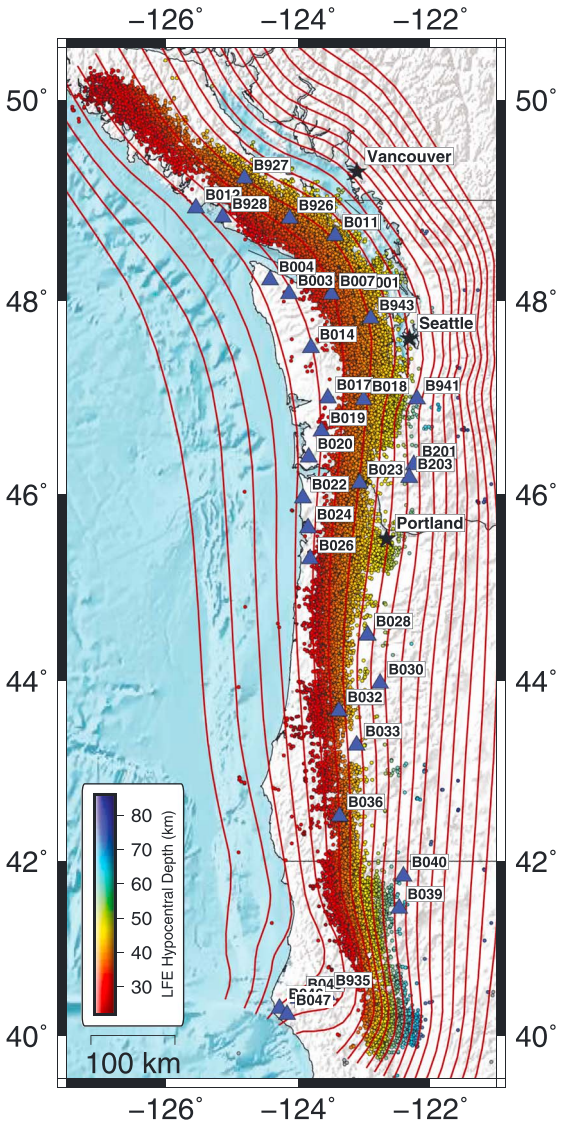

Figure 1. Distribution of tremor epicenters for the episodic tremor and slip episodes of 2009, 2012, and 2015–2016, colored by hypocentral depth. Stations used in this study are marked with blue triangles. Slab depth contours from the McCrory et al. (2012) slab model are delineated with red lines, in 5-km intervals.

motion using a basic GMPE, describing the PGA A_{ij} from each event i at station j as a combination of its initial amplitude A_{i0}, geometric spreading $1/R_{ij}$, a site term S_j, and anelastic attenuation (equation (1)):

$$A_{ij} = A_{i0} \exp\left(\frac{-\pi f R_{ij}}{Q\beta}\right) \frac{1}{R_{ij}} S_j \tag{1}$$

The anelastic attenuation parameter is defined as $C2 \equiv \frac{\pi f}{Q\beta}$ (e.g., Abrahamson et al., 2014), where f is frequency, β is the shear wave velocity, and Q the quality factor. We note that we fix geometrical spreading in equation (1) to be R^{-1}; however, empirically derived ground motion attenuation models often find exponents other than −1 (e.g., Abrahamson et al., 2014; Atkinson & Mereu, 1992; Fatehi & Hermann, 2008). In solving for attenuation there is a strong trade-off between geometrical spreading and anelastic attenuation terms, where a larger geometrical spreading term, such as $R^{-1.3}$, would imply a smaller attenuation term.

We begin by taking the natural log of equation (1) and define relative magnitude terms $C1_i \equiv lnA_{i0}$. To alleviate the need to solve for an initial amplitude A_{i0} directly, we compare recorded amplitudes from each event for each station pair. In doing so, the common initial amplitude term is temporarily eliminated and we can

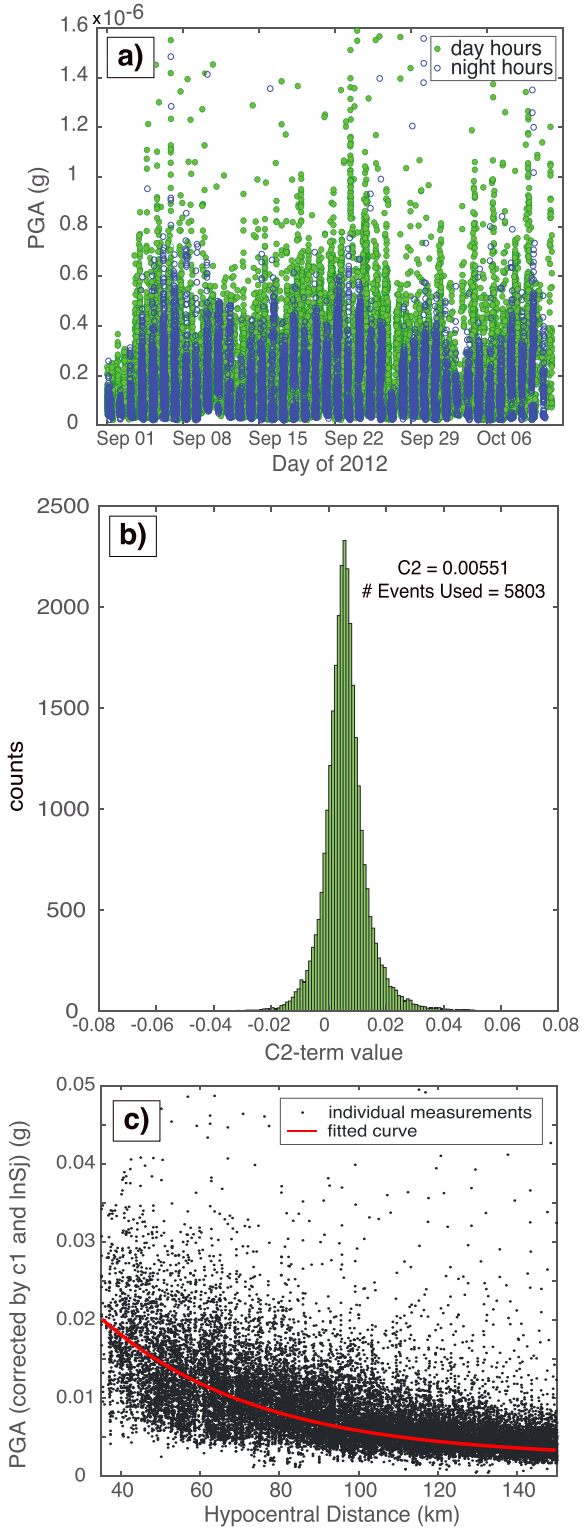

Figure 2. (a) Tremor PGA amplitudes for the 2012 ETS episode. Daytime amplitudes (green) are generally larger than those at night (blue), reflecting the effect of anthropogenic noise on tremor amplitudes. (b) Distribution of *C*2 terms for the entire data set, after limiting to the largest 10% of events occurring during a 7-hr nighttime window and within the 150-km hypocentral distance restriction. (c) PGA amplitudes plotted with distance for the entire data set, corrected with relative source and site terms, $C1_i$ and lnS_j, obtained from the inversion. PGA = peak-ground acceleration; ETS = episodic tremor and slip.

Table 1
Comparison of C2 Values Found in This Study to Those of Atkinson and Boore (1997)

Frequency band (Hz)	PGA C2 term	Q	Frequency (Hz)	AB (1997) C4 term
1–3	0.00420	219–657	1.3	0.00345
			2.0	0.00414
2–6	0.00544	338–1,015	3.2	0.00530
			5.0	0.00645
3–9	0.00788	350–1,051	8.0	0.00783
			10	0.00829

Note. Q is computed using $\beta = 3.4147\ \frac{km}{s}$ (average crustal value at latitude 46.75°, longitude −123.75°, from Shen et al., 2013). PGA = peak-ground acceleration.

determine an initial estimate of $C2$ as the least squares solution. We then use the preliminary $C2$ to solve for the relative magnitude terms $C1_i$ and site terms S_j, which are kept in natural log form. Finally, we solve again for $C2$ using all previously determined parameters and take the sample median (equation (2) and Figure 2b).

$$C2 = \frac{lnA_{ij} - lnS_j - C1_i + lnR_{ij}}{-R_{ij}} \tag{2}$$

PGA attenuation for the final data set, corrected for $C1_i$ and site terms S_j, is plotted in Figure 2c, according to equation (3):

$$\text{Corrected } A_{ij} = \exp(lnA_{ij} - C1_i - lnS_j) \tag{3}$$

PGA amplitudes for the 2012 ETS episode (Figure 2a) are overall slightly larger than those in 2009 and 2015–2016. However, because we correct for relative magnitude terms ($C1$) in the inversion, the attenuation term does not vary significantly between ETS episodes of different estimated seismic moment.

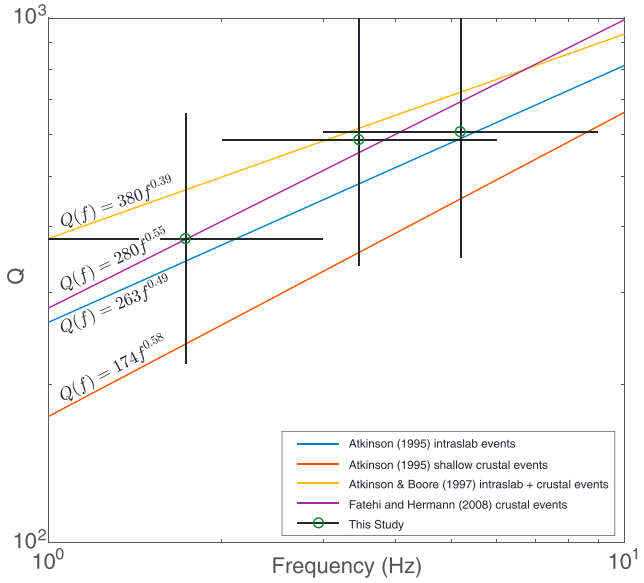

Figure 3. Comparison of our results for Q, in black lines, with existing frequency-dependent Q models in Cascadia (Atkinson, 1995; Atkinson & Boore, 1997; Fatehi & Hermann, 2008). Cross and green circles denote frequency bands and associated ranges of Q and the middle value, respectively. Whereas Atkinson and Boore (1997) do not differentiate between intraslab and crustal earthquakes in their analysis (yellow line), Atkinson (1995) found attenuation relations for shallow crustal earthquakes (depth < 10 km; red line) and lower crustal and intraslab earthquakes (20 < depth < 30 km; blue line). Fatehi and Hermann (2008) used crustal earthquakes of magnitude ≥ 3 (purple line).

To explore the relationship of attenuation and frequency in tremor, we refilter our data set in 1- to 3-Hz, 2- to 6-Hz, and 3- to 9-Hz frequency bands (equal bandwidths in log-space) and reprocess the PGA data as described above. We repeat the inversion for $C2$ to solve for the attenuation parameter in each frequency band.

To test spatial variation of the attenuation parameter, we grid the Cascadia margin in 1-square-degree latitude by longitude cells and compute raypaths for each station-event pair. Data for the events corresponding to each raypath through the cell are used to invert for the attenuation parameter. To cover all of Cascadia, the 1-square-degree cell bounds are shifted in 0.1° latitude or longitude increments along the entire margin. Because many cells near edges of the study region are sparse, we set a threshold of a minimum of 500 raypaths for the inversion in each cell. We invert for $C2$ in each cell to find a spatially varying attenuation term, over the full frequency band of 1–10 Hz.

3. Results

Overall, we find a median $C2 = 0.00551$ for the entire data set in the full 1- to 10-Hz bandwidth. For reference, in Cascadia, Baltay and Beroza (2013) found $C2 = 0.00647$ using PGA of tremor. It is worth noting that our tremor source region extends much farther south through Oregon compared to that study. Additionally, we estimate hypocentral depths using the McCrory et al. (2012) Juan de Fuca slab model, whereas Baltay and Beroza (2013) used a constant 30-km hypocentral depth. Hence, we attribute the difference in $C2$ values to different tremor source-to-site paths.

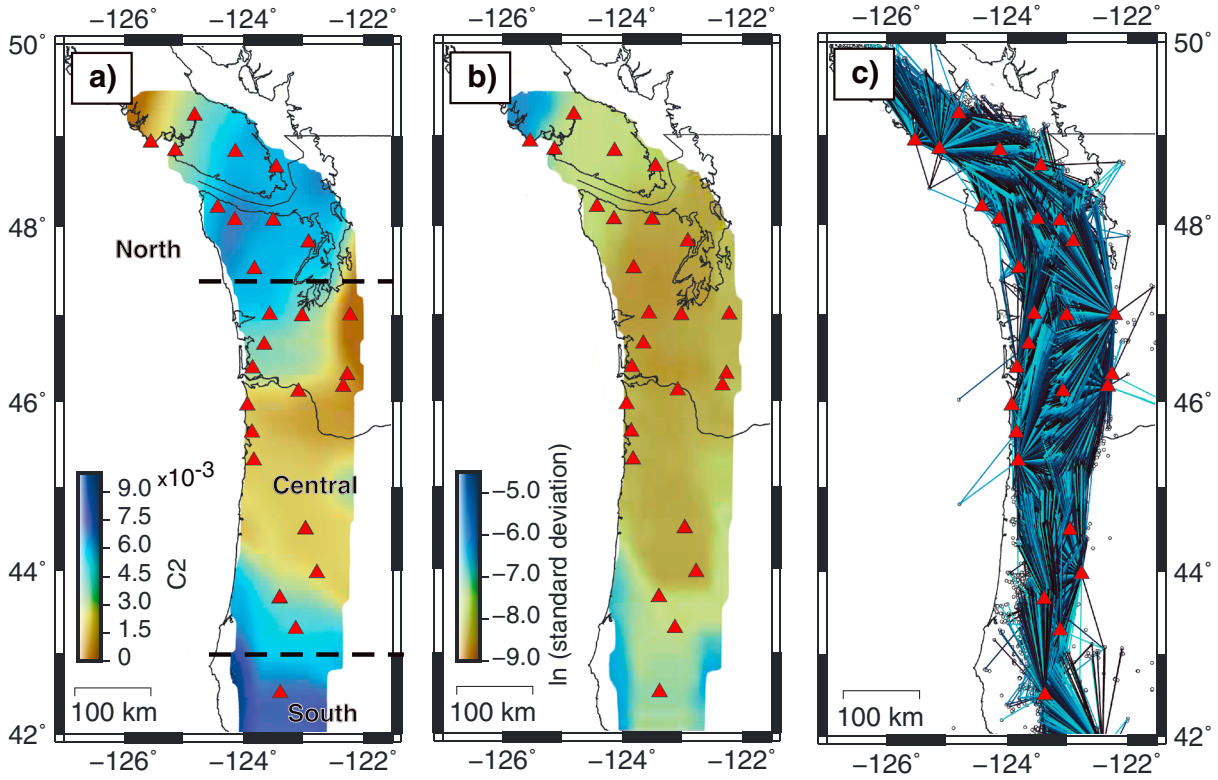

Figure 4. Map with (a) $C2$ from the inversion, with blue indicating areas of higher attenuation ($C2 \propto \frac{1}{Q}$). (b) Associated standard deviation of $C2$ values computed from the bootstrapping test, in log scale. (c) Raypaths for each station-event pair for all events used. Red triangles indicate Plate Boundary Observatory stations. Horizontal dashed lines indicate general boundaries of Cascadia segments, from Brudzinski and Allen (2007). Due to insufficient station coverage close to tremor hypocenters in southern Cascadia, we are unable to solve for $C2$ in most of this region. (Figures were smoothed with a Gaussian filter).

3.1. Frequency Dependence of Attenuation

The region with latitude bounds 45–49° affords the best coverage of stations close to tremor epicenters in Cascadia (Figure 1), so we use data within this region to analyze frequency dependence of the attenuation parameter. Inversion in each frequency band 1–3, 2–6, and 3–9 Hz shows that $C2$ increases with frequency, in a manner consistent with existing models of attenuation in Cascadia (Table 1 and Figure 3). For the 1- to 3-Hz data set we find $C2 = 0.00420$; for 2–6 Hz, $C2 = 0.00544$; and for 3–9 Hz, $C2 = 0.00788$. Q is often represented as $Q = Q_0 f^{\alpha}$, where typically $0 \leq \alpha \leq 1$ ($\alpha = 0$ implies a frequency-independent attenuation; e.g., Aki, 1980; Atkinson & Mereu, 1992). Inputting our obtained values for $C2$ into $C2 \equiv \frac{\pi f}{Q\beta}$ allows us to compare our corresponding Q values to existing $Q(f)$ relations for Cascadia (Figure 3). We estimate $\beta = 3.4147 \frac{\text{km}}{\text{s}}$ by taking the average shear wave velocity V_s from 0- to 30-km depth at latitude 46.75°, longitude −123.75° from the 3-D shear wave velocity model of Shen et al. (2013). Our values for $C2$ in each frequency band (1–3, 2–6, and 3–9 Hz) correspond to Q ranges of 219–657, 338–1015, and 350–1,051, respectively. Atkinson and Boore (1997) used a stochastic point source model to find the attenuation parameter ($C4$ in their study) and $Q(f) = 380f^{0.39}$, whereas Atkinson (1995) used regression analysis to find $Q(f) = 263f^{0.49}$ for lower crustal and intraslab earthquakes (20 km < depth < 30 km) and $Q(f) = 174f^{0.58}$ for shallow crustal earthquakes (depth ≤ 10 km). Both studies utilized intraslab and crustal earthquakes of moderate to large magnitudes ($M_w \sim 3 - 8$). Fatehi and Hermann (2008) also employed regression analysis to fit $Q(f) = 280f^{0.55}$ in Cascadia using peak-ground velocity amplitudes of predominantly crustal earthquakes of magnitude $M >= 3$. Our data estimates for Q using tremor lie between the $Q(f)$ relations for all three studies (Figure 3).

3.2. Spatial Variation of Attenuation

Our results show significant spatial variability in seismic wave attenuation in Cascadia, primarily along strike (Figure 4). Due to the narrow station and data distribution which is limited to the tremor source region of 25- to 45-km depth, we only interpret along-strike variations in $C2$. We consider three general regions, calculating the median $C2$ value within each. The attenuation parameter reaches its highest values (i.e., greatest

attenuation and thus smallest Q) in northern Cascadia from ~47–49° latitude, with a median value of $C2 = 0.00667$ (standard deviation = 0.0094; supporting information Figure S1). The attenuation parameter decreases within latitudes 43–47° in central Cascadia, with a median of $C2 = 0.00279$ (standard deviation = 0.0066), then increases again in southern Oregon (median $C2 = 0.00723$, standard deviation = 0.011). A two-sample t test at a 5% significance level demonstrates that the northern Cascadia and southern Oregon regions come from distributions with different means from central Cascadia, that is, the regions have statistically significant differences in $C2$. While many stations in Washington state and Vancouver Island are very close to tremor epicenters, the station distribution becomes increasingly sparse in central and southern Oregon and northern California, where the closest recordings are at a minimum of 60–70 km for some stations (supporting information Figure S2). Consequently, results for $C2$ are more variable in southern Cascadia.

We estimate model uncertainties by performing a bootstrap test (Efron & Tibshirani, 1993). We first generate 100 new data sets by resampling the original tremor data set with replacement, then reinvert for $C2$ in each 1-square-degree cell along the entire Cascadia margin for each resampled data set. Standard deviations are computed from the $C2$ values from all 100 data sets (Figure 4b). Values are lowest from latitudes 44–49, where station coverage and tremor density are highest.

4. Discussion

In the results section we demonstrated that tectonic tremor can be used in a ground motion framework to estimate spatial variations in and the frequency dependence of crustal attenuation in Cascadia. To ascertain whether variations in β or Q are primarily responsible for our observed variations in $C2$, we take representative values of β for the north, central, and southern regions using the shear wave velocity model of Shen et al. (2013). Using representative values of $C2$ for each region and the definition of $C2$ from section 3.1, we find that variations in β alone are insufficient to account for apparent variations in $C2$; differences in Q along the Cascadia forearc are required. We also find that $C2$ generally increases with frequency in a manner that is consistent with the findings of previous studies that employed different sources (Table 1). Hence, nonvolcanic tremor and other small magnitude sources may be beneficial in estimating regional GMPE parameters.

Crustal attenuation of seismic waves is largely controlled by fluid content and rock permeability (Mavko & Nur, 1979; Mitchell, 1995; Winkler & Nur, 1979). The presence of fluids in crustal rocks affects attenuation due to relative motion between fluids that occupy pore space and the solid matrix, resulting in viscous dissipation of energy (Mavko & Nur, 1979; Mavko et al., 1979; O'Connell & Budiansky, 1977). Thus, rock permeability controls the ability of fluids to move between pore spaces, and increased permeability enhances shear energy losses by allowing fluid flow (Mavko & Nur, 1979). Laboratory experiments on dry rock generally find frequency-independent Q, and with the addition of fluids, attenuation is greatly increased and stronger frequency dependence is observed (Knopoff, 1964; Winkler & Nur, 1982). Because we observe frequency-dependent $C2$, and differences in $C2$ are largely controlled by differences in Q, the variations in $C2$ along the margin likely reflect differences in fluid content in the forearc.

It is well established that Cascadia is segmented with north, central, and southern sections that are physically distinct. This segmentation is present in the upper mantle velocity structure (Bodmer et al., 2018), variations in plate coupling (Schmalzle et al., 2014), and density and recurrence intervals of nonvolcanic tremor and ETS events, respectively (Boyarko & Brudzinski, 2010; Brudzinski & Allen, 2007), along-strike extent of megathrust earthquakes (Goldfinger et al., 2012), lithology (Trehu et al., 1994), and topography. Our results show that this segmentation also manifests in the forearc attenuation structure. We find that areas of high attenuation (i.e., north of latitude ~47°, south of latitude ~43°; Figure 4a) correspond to regions with increased tremor density and frequency of ETS recurrence (Brudzinski & Allen, 2007). Various structural controls on fluid mobility through the forearc crust have been proposed to explain along-strike variations in ETS behavior (Audet et al., 2009; Audet & Burgmann, 2014; Hyndman et al., 2015; Wells et al., 2017). Of relevance to our results are the findings of Hansen et al. (2012), who used teleseismic receiver functions in four different locations along the Cascadia forearc to estimate ratios of compressional P wave velocity to shear S wave velocity $\left(\frac{V_p}{V_s}\right)$, which are a function of the Poisson ratio and thought to reflect fluid content. They find that the Siletz terrane in central Cascadia has higher $\frac{V_p}{V_s}$ ratios in both the crust and low-velocity zone than the adjacent Wrangellia and Klamath terranes (northern and southern Cascadia, respectively). In principle, higher $\frac{V_p}{V_s}$ should imply higher attenuation, yet comparison of our $C2$ values with their $\frac{V_p}{V_s}$ ratios indicates the opposite, as Hansen et al.

(2012) find slightly higher $\frac{V_p}{V_s}$ in central Cascadia relative to northern and southern Cascadia. We attribute this apparent inconsistency to the disparate frequency contents employed in each study (1–10 Hz, as opposed to 0.03–0.5 Hz; Hansen et al., 2012), which are sensitive to different length scales. As such, our analysis should be sensitive to smaller-scale structure. If this interpretation is correct, variations in attenuation determined from tremor may arise from a localized fluid source within the crust, possibly controlled by variable structural properties of the crustal forearc along strike (e.g., Audet & Burgmann, 2014; Hyndman et al., 2015; Wells et al., 2017). Furthermore, our results lend support to the notion that along-strike variations in crustal fluid distribution exert a key control on the occurrence of ETS.

5. Conclusions

By applying the inversion method of Baltay and Beroza (2013) using tremor amplitudes, we determine a regionally varying attenuation parameter in Cascadia, with lower average values in central Cascadia relative to those above latitude ~47° and south of latitude ~43°. We consider the possibility that spatial variations are a manifestation of varying crustal fluid content throughout Cascadia, although we are not able to determine the relative importance of different physical factors. In addition, we see a dependence of the attenuation parameter with frequency, in accordance with existing attenuation parameters in GMPEs developed for Cascadia. Consistency of our average and frequency-dependent attenuation values with those in existing GMPEs in Cascadia validates the use of tremor for improvements in ground motion modeling. This can be very helpful in regions such as Cascadia where moderate-to-large earthquakes are sparse and thus observational constraints on attenuation are lacking. Finally, the results of this study can be integrated with other geophysical findings to elucidate the relationship between physical properties of the forearc and earthquake behavior in Cascadia, which is imperative for understanding subduction zone seismogenesis and resulting implications for hazard assessment.

Acknowledgments

The Interactive Tremor Map of the Pacific Northwest Seismic Network provided tremor epicenters and dates (Wech & Creager, 2008). The facilities of IRIS Data Services, and specifically the IRIS Data Management Center, were used for access to waveforms used in this study. IRIS Data Services are funded through the Seismological Facilities for the Advancement of Geoscience and EarthScope (SAGE) Proposal of the National Science Foundation under Cooperative Agreement EAR-1261681. Ground motion data were recorded on Plate Boundary Observatory borehole stations, an EarthScope initiative, funded by the National Science Foundation. Figures 1 and 4 were produced using the Generic Mapping Tools package (Wessel et al., 2013). The authors appreciate insightful discussion with Emilie Hooft and Eugene Humphreys and constructive comments from Patricia McCrory, Jack Boatwright, and two anonymous reviewers. This work was funded by a Vice President for Research and Innovation (VPRI) fellowship and Mini-Grant through the University of Oregon to G. F. L. and National Science Foundation grant EAR-1520238 to A. M. T.

References

Abrahamson, N. A., Silva, W. J., & Kamai, R. (2014). Summary of the ASK14 ground-motion relation for active crustal regions. *Earthquake Spectra*, *30*(3), 1025–1055. https://doi/org/10.1193/070913EQS198M

Aki, K. (1980). Scattering and attenuation of shear waves in the lithosphere. *Journal of Geophysical Research*, *85*(B11), 6496–6504.

Atkinson, G. M. (1995). Attenuation and source parameters of earthquakes in the Cascadia region. *Bulletin of the Seismological Society of America*, *85*(5), 1327–1342.

Atkinson, G. M., & Boore, D. (1997). Stochastic point-source modeling of ground motions in the Cascadia region. *Seismological Research Letters*, *68*(1), 74–85.

Atkinson, G. M., & Mereu, R. F. (1992). The shape of ground motion attenuation curves in southeastern Canada. *Bulletin of the Seismological Society of America*, *82*(5), 2014–2031.

Atwater, B. F. (1995). Summary of coastal geologic evidence for past great earthquakes at the Cascadia subduction zone. *Earthquake Spectra*, *11*(1), 1–18. https://doi.org/10.1785/0120140032

Atwater, B. F., Carson, B., Griggs, G. B., Johnson, H. P., & Salmi, M. S. (2014). Rethinking turbidite paleoseismology along the Cascadia subduction zone. *Geology*, *42*(9), 827–830. https://doi.org/10.1130/G35902.1

Audet, P., Bostock, M. G., Christensen, N. I., & Peacock, S. M. (2009). Seismic evidence for overpressured subducted oceanic crust and megathrust fault sealing. *Nature*, *467*, 76–78. https://doi.org/10.1038/nature07650

Audet, P., & Burgmann, R. (2014). Possible control of subduction zone slow-earthquake periodicity by silica enrichment. *Nature*, *510*, 389–392. https://doi.org/10.1038/nature13391

Baltay, A. S., & Beroza, G. C. (2013). Ground-motion prediction from tremor. *Geophysical Research Letters*, *40*, 6340–6345. https://doi.org/10.1002/2013GL058506

Bodmer, M., Toomey, D. R., Hooft, E. E., & Schmandt, B. (2018). Buoyant asthenosphere beneath Cascadia influences megathrust segmentation. *Geophysical Research Letters*, *45*, 6954–6962. https://doi.org/10.1029/2018GL078700

Bostock, M. G., Thomas, A. M., Rubin, A. M., & Christensen, N. I. (2017). On corner frequencies, attenuation, and low-frequency earthquakes. *Journal of Geophysical Research: Solid Earth*, *122*, 543–557. https://doi.org/10.1002/2016JB013405

Bostock, M. G., Thomas, A. M., Savard, G., Chuang, L., & Rubin, A. M. (2015). Magnitudes and moment-duration scaling of low-frequency earthquakes beneath southern Vancouver Island. *Journal of Geophysical Research: Solid Earth*, *120*, 6329–6350. https://doi.org/10.1002/2015JB012195

Boyarko, D. C., & Brudzinski, M. R. (2010). Spatial and temporal patterns of nonvolcanic tremor along the southern Cascadia subduction zone. *Journal of Geophysical Research*, *115*, B00A22. https://doi.org/10.1029/2008JB006064

Brown, J. R., Beroza, G. C., Ide, S., Ohta, K., Shelly, D. R., Schwartz, S. Y., et al. (2009). Deep low-frequency earthquakes in tremor localize to the plate interface in multiple subduction zones. *Geophysical Research Letters*, *36*, L19306. https://doi.org/10.1029/2009GL040027

Brudzinski, M. R., & Allen, R. M. (2007). Segmentation in episodic tremor and slip all along Cascadia. *Geology*, *35*(10), 907–910. https://doi.org/10.1130/G23740A

Dragert, H., Wang, K., & James, T. S. (2001). A silent slip event on the deeper Cascadia subduction interface. *Science*, *292*(5521), 1525–1528.

Efron, B., & Tibshirani, R. J. (1993). *An introduction to the bootstrap*. New York: Chapman and Hall.

Fatehi, A., & Hermann, R. B. (2008). High-frequency ground-motion scaling in the Pacific Northwest and in Northern and Central California. *Bulletin of the Seismological Society of America*, *98*(2), 709–721. https://doi.org/10.1785/0120070051

Goldfinger, C., Nelson, C., Morey, A., Johnson, J., Patton, J., Karabanov, E., et al. (2012). Turbidite event history—Methods and implications for Holocene paleoseismicity of the Cascadia subduction zone. *U.S. Geological Survey Professional Paper 1661-F*, 170. https://pubs.usgs.gov/pp/pp1661f/

Gomberg, J., Creager, K., Sweet, J., Vidale, J., Ghosh, A., & Hotovec, A. (2012). Earthquake spectra and near-source attenuation in the Cascadia subduction zone. *Journal of Geophysical Research*, *117*, B05312. https://doi.org/10.1029/2011JB009055

Hanks, T. C., & McGuire, R. K. (1981). The character of high-frequency strong ground motion. *Bulletin of the Seismological Society of America*, *71*(6), 2071–2095.

Hansen, R. T. J., Bostock, M. G., & Christensen, N. I. (2012). Nature of the low velocity zone in Cascadia from receiver function waveform inversion. *Earth and Planetary Science Letters*, *337-338*, 25–38. https://doi.org/10.1016/j.epsl.2012.05.031

Hyndman, R. D., McCrory, P. A., Wech, A., Kao, H., & Ague, J. (2015). Cascadia subducting plate fluids channelled to fore-arc mantle corner: ETS and silica deposition. *Journal of Geophysical Research: Solid Earth*, *120*, 4344–4358. https://doi.org/10.1002/2015JB011920

Ide, S., Shelly, D. R., & Beroza, G. C. (2007). Mechanism of deep low frequency earthquakes: Further evidence that deep non-volcanic tremor is generated by shear slip on the plate interface. *Geophysical Research Letters*, *34*, L03308. https://doi.org/10.1029/2006GL028890

Knopoff, L. (1964). Q. *Reviews of Geophysics*, *2*(4), 625–660. https://doi.org/10.1029/RG002i004p00625

Mavko, G., Kjartansson, E., & Winkler, K. (1979). Seismic wave attenuation in rocks. *Reviews of Geophysics*, *17*(6), 1155–1164.

Mavko, G. M., & Nur, A. (1979). Wave attenuation in partially saturated rocks. *Geophysics*, *44*(2), 161–178.

McCrory, P. A., Blair, J. L., Waldhauser, F., & Oppenheimer, D. H. (2012). Juan de Fuca slab geometry and its relation to Wadati-Benioff zone seismicity. *Journal of Geophysical Research*, *117*, B09306. https://doi.org/10.1029/2012JB009407

Miller, M. M., Melbourne, T., Johnson, D. J., & Sumner, W. Q. (2002). Periodic slow earthquakes from the Cascadia subduction zone. *Science*, *295*(5564), 2423. https://doi.org/10.1126/science.1071193

Mitchell, B. J. (1995). Anelastic structure and evolution of the continental crust and upper mantle from seismic surface wave attenuation. *Reviews of Geophysics*, *33*(4), 441–462. https://doi.org/10.1029/95RG02074

O'Connell, R. J., & Budiansky, B. (1977). Viscoelastic properties of fluid-saturated cracked solids. *Journal of Geophysical Research*, *82*(36), 5719–5735.

Obara, K. (2002). Nonvolcanic deep tremor associated with subduction in southwest Japan. *Science*, *296*(5573), 1679–1681.

Petersen, M. D., Moschetti, M. P., Powers, P. M., Mueller, C. S., Haller, K. M., Frankel, A. D., et al. (2014). Documentation for the 2014 update of the United States National Seismic Hazard Maps. *U.S. Geological Survey Open-File Report 2014-1091*, 243. https://doi.org/10.3133/ofr20141091

Rogers, G., & Dragert, H. (2003). Episodic tremor and slip on the Cascadia subduction zone: The chatter of silent slip. *Science*, *300*(5627), 1942–1943.

Royer, A. A., & Bostock, M. G. (2014). A comparative study of low frequency earthquake templates in northern Cascadia. *Earth and Planetary Science Letters*, *402*, 247–256. https://doi.org/10.1016/j.epsl.2013.08.040

Satake, K., Shimazaki, K., Tsuji, Y., & Ueda, K. (1996). Time and size of a giant earthquake in Cascadia inferred from Japanese tsunami records of January 1700. *Nature*, *379*(6562), 246–249.

Satake, K., Wang, K., & Atwater, B. F. (2003). Fault slip and seismic moment of the 1700 Cascadia earthquake inferred from Japanese tsunami descriptions. *Journal of Geophysical Research*, *108*(B11), 2535. https://doi.org/10.1029/2003JB002521

Schmalzle, G., McCaffrey, R., & Creager, K. C. (2014). Central Cascadia subduction zone creep. *Geochemistry, Geophysics, Geosystems*, *15*, 1515–1532. https://doi.org/10.1002/2013GC005172

Shelly, D., Beroza, G. C., & Ide, S. (2007). Non-volcanic tremor and low-frequency earthquake swarms. *Nature*, *446*(7133), 305–307. https://doi.org/10.1038/nature05666

Shelly, D., Beroza, G. C., Ide, S., & Nakamula, S. (2006). Low-frequency earthquakes in Shikoku, Japan, and their relationship to episodic tremor and slip. *Nature*, *442*, 188–191. https://doi.org/10.1038/nature04931

Shen, W., Ritzwoller, M. H., & Schulte-Pelkum, V. (2013). A 3-D model of the crust and uppermost mantle beneath the Central and Western US by joint inversion of receiver functions and surface wave dispersion. *Journal of Geophysical Research*, *118*, 262–276. https://doi.org/10.1029/2012JB009602

Trehu, A., Asudeh, I., Brocher, T., Luetgert, J., Mooney, W., Nabelek, J., & Nakamura, Y. (1994). Crustal architecture of the Cascadia forearc. *Science*, *266*(5183), 237–243. https://doi.org/10.1126/science.266.5183.237

Wech, A. G., & Creager, K. C. (2008). Automatic detection and location of Cascadia tremor. *Geophysical Research Letters*, *35*, L20302. https://doi.org/10.1029/2008GL035458

Wells, R. E., Blakely, R. J., Wech, A. G., McCrory, P. A., & Michael, A. (2017). Cascadia subduction tremor muted by crustal faults. *Geology*, *45*(6), 515–518. https://doi.org/10.1130/G38835.1

Wessel, P., Smith, W. F., Scharroo, R., Luis, J., & Wobbe, F. (2013). Generic Mapping Tools: Improved version released. *Eos Transactions*, *94*(45), 409–410.

Winkler, K., & Nur, A. (1979). Pore fluids and seismic attenuation in rocks. *Geophysical Research Letters*, *6*(1), 1–4. https://doi.org/10.1029/RG028i004p00399

Winkler, K. W., & Nur, A. (1982). Seismic attenuation: Effects of pore fluids and frictional sliding. *Geophysics*, *47*(1), 1–15. https://doi.org/10.1190/1.1441276

Yabe, S., Baltay, A. S., Ide, S., & Beroza, G. C. (2014). Seismic-wave attenuation determined from tectonic tremor in multiple subduction zones. *Bulletin of the Seismolgical Society of America*, *104*(4), 2043–2059.